1   ***Title***

2   Estimation of soil splash detachment rates on the forest floor of an unmanaged Japanese cypress

3   plantation based on field measurements of throughfall drop sizes and velocities

4   ***Authors***

5   Kazuki Nanko[a] [*], Shigeru Mizugaki[a, b], Yuichi Onda[a]

6   [a] *Department of Integrative Environmental Sciences, Graduate School of Life and*

7   *Environmental Sciences, University of Tsukuba, Ten-nodai 1-1-1, Tsukuba-shi, Ibaraki,*

8   *305-8577, Japan*

9   [b] *Japan Science and Technology Agency, Japan*

10

11   ***Abstract***

12   To study and model the interrill erosion process in an unmanaged Japanese cypress

13   (*Chamaecyparis obtusa*) plantation, soil splash detachment rates were estimated based on the

14   quantification of throughfall raindrop indices. Throughfall drops and soil splash detachment

15   were simultaneously observed in the field, and observed data were compared with estimates

16   produced by previous models. Observations took place over five months in 2005, during six

17   observation periods. Raindrop indices of kinetic energy (KE), momentum (M), and momentum

18   multiplied by the drop diameter (MD) were calculated from drop diameters and velocities. The

[*] Corresponding author. Tel & Fax: +81-29-853-6878
E-mail: knanko@geoenv.tsukuba.ac.jp / nanko-kazuki@gi.main.jp (K. Nanko).

1 median volume diameter of 1.99 mm for the overall observation period was well bounded by

2 those from other Japanese cypress plantations. Throughfall consisted of large drops, generated

3 as drips, exceeding 3 mm in diameter. The fall height was insufficient for the drops to attain

4 terminal velocity, with 91% of the drops reaching less than 90% terminal velocity. The observed

5 throughfall raindrop indices had strong correlation with throughfall rainfall intensity, even

6 though throughfall raindrops occurred in seven rainfall events with different meteorological

7 conditions. The values of observed KE and M were lower than previous model-derived

8 estimations. Earlier models tended to overestimate throughfall KE and M, partly because the

9 expected velocity was greater than that observed, and partly because they did not consider the

10 effect of the splash water component during throughfall. The splash detachment rate in forests

11 was weakly correlated with the total-amount raindrop indices but strongly correlated with the

12 maximum value of raindrop indices over a short time scale such as 1 h. This result indicates that

13 continuous and concentrated raindrop impacts over a short time duration cause splash

14 detachment in the forest floor. Development of a comprehensive model of the process of forest

15 floor soil surface erosion requires more detailed measurement of actual throughfall drops.

16

19

1. Introduction

Numerous studies have focused on soil loss from agricultural lands around the world. In Japan, soil erosion on forested slopes is a serious problem, especially in unmanaged forest plantations of Japanese cypress (*Chamaecyparis obtusa*), a major commercial tree species (e.g., Akenaga and Shibamoto, 1933; Kawana et al., 1963; Miura et al., 2002). Interrill erosion generally does not occur in forested areas because forest litter and understory vegetation form a protective surface cover. However, unmanaged Japanese cypress plantations have little surface cover, in part because cypress litter can easily break into small pieces after falling to the ground (Sakai and Inoue, 1988) and then be washed away (Hattori et al., 1992). Furthermore, the weak penetration of sunlight into forest plantations results in poor growth of understory vegetation (Kiyono, 1990).

In such forests, the impact of raindrops can break the aggregated structure of the A_0 horizon. Subsequently, the infiltration rate decreases (Yukawa and Onda, 1995), and Horton overland flow may be generated during large rainstorms (Tsujimura et al., 2006). Similar erosion problems have been observed in other types of plantations, including eucalyptus (*Eucalyptus exserta*) plantations in southern China (Zhou et al., 2002), southern India (Calder et al., 1993), and northern Portugal (Terry, 1996); teak (*Tectona grandis*) plantations in southern India (Calder, 2001); and coffee plantations in the tropics (Hanson et al., 2004). Control of soil erosion is important for sustaining the long-term productivity of natural resources and for protecting aquatic ecosystems.

3

1   Soil splash detachment is the initial process in interrill erosion in the sequence leading to

2   soil loss and subsequent sediment transport (e.g., Ellison, 1944; van Dijk et al., 2002b; Kinnel,

3   2005). Some physically based models of soil erosion processes such as the

4   Morgan–Morgan–Finney (Morgan et al., 1984, revised by Morgan, 2001) and EUROSEM

5   (Morgan et al., 1998) models have incorporated soil splash detachment triggered by the raindrop

6   impact onto the soil surface. Kinetic energy has widely been used as the raindrop index

7   controlling soil splash detachment (Mihara, 1951; Free, 1960; Quansah, 1981; Poesen, 1985;

8   Al-Durrah and Bradford, 1988; Morgan et al., 1998), although other suggested indices have

9   included raindrop momentum (Rose, 1960; Park et al., 1983) or the kinetic energy and drop

10   circumference (Govers, 1991). Salles and Poesen (2000) reported that the momentum

11   multiplied by the drop diameter was the best raindrop index for soil splash detachment.

12   However, no study has estimated the soil splash detachment by several raindrop indices in field

13   measurements.

14   In Japanese cypress plantations, soil splash detachment is believed to be a predominant

15   factor contributing to interrill erosion (Miura et al., 2002). Owing to canopy effects, the

16   characteristics of throughfall raindrops differ from those of open rainfall. Throughfall consists

17   of three drop components: free throughfall, drips, and splash water droplets (Nanko et al., 2006).

18   Usually, compared with open rainfall, throughfall drops are larger in size because of drips

19   (Chapman, 1948; Nanko et al., 2004) and are fewer in number (Nanko et al., 2004). Additionally,

20   throughfall drops' velocities are generally lower than the terminal velocity (Laws, 1941; Wang

4

1 and Pruppacher, 1977) because of the shorter fall height. Throughfall drops thus have unstable

2 shapes varying between prolate and oblate (Epema and Riezebos, 1984), with prolate drops

3 having larger erosivity than oblate drops (Riezebos and Epema, 1985). These characteristics

4 cause throughfall raindrops to have different erosive potential compared with open rainfall.

5 Therefore, quantification of throughfall drop indices and soil splash detachment rates at the

6 forest floor are required to study and model the interrill erosion process in unmanaged Japanese

7 cypress plantations. However, few studies have collected these data.

8 First, no studies have measured actual throughfall drop velocities under canopies. The

9 calculation of raindrop indices requires the size and velocity measurements of raindrops. Many

10 researchers have measured the drop size distribution (DSD) of throughfall and leafdrips using

11 field observations and laboratory experiments (Chapman, 1948; Mosley, 1982; Vis, 1986;

12 Brandt, 1989; Zhou et al., 2002; Nanko et al., 2006). Studies of mature forests with sufficient

13 canopy height, including Japanese cypress plantations (Nanko et al., 2004) and other canopy

14 species (Chapman, 1948; Tsukamoto, 1966; Brandt, 1989; Zhou et al., 2002), have found that

15 throughfall has greater kinetic energy than open rainfall because the canopies produce larger

16 drops as leafdrips. However, these studies assumed drop velocity using empirical or theoretical

17 calculations from previous studies (*e.g.*, Laws, 1941; Gunn and Kinzer, 1949; van Dijk et al.,

18 2002a). The Brandt model (Brandt, 1990), which was the only available model for calculating

19 the kinetic energy and the momentum of throughfall, also relied on assumptions in calculating

20 leafdrip drop velocity.

5

1   Second, few studies have quantified soil splash detachment rates in forests. In Japan,

2 researchers have mainly used sediment traps (described by Tsukamoto, 1991) to estimate soil

3 surface erosion at the forest floor (*e.g.*, Miura et al., 2002). Sediment traps are easy to set up, and

4 their measurement method is simple. However, they are unable to evaluate soil splash

5 detachment rates for two reasons: they catch soil particles produced by both raindrop impact and

6 overland flow, and they measure the sediment transport rate ($g\ m^{-1}$) instead of the soil splash

7 detachment rate ($g\ m^{-2}$) because they are generally set without plot-bordering. Although the

8 transport rate is important for understanding sediment movement phenomena, it cannot be

9 incorporated into a soil erosion process model. In contrast, research in other countries has

10 measured soil splash detachment rates in forested areas; Terry (1996) used splash funnels in a

11 eucalyptus plantation in northern Portugal, and Vis (1986) used sand-filled splash cups in a

12 tropical Columbian rainforest. However, they were unable to measure throughfall drop indices

13 and only revealed soil splash detachment rate ($g\ m^{-2}$) or soil splash detachment rate per unit

14 rainfall ($g\ m^{-2}\ mm^{-1}$). No studies have estimated soil splash detachment rates in forested areas

15 based on the quantification of throughfall drop indices.

16   The objective of this study, therefore, was to estimate the soil splash detachment rate in an

17 unmanaged Japanese cypress plantation based on quantification using throughfall drop indices.

18 First, we determined the characteristics of throughfall drops, the DSD, and the drop velocity.

19 Second, we estimated the soil splash detachment rate in forests using throughfall drop indices.

20 Third, we compared actual measured data with estimates from previous models.

1

2. Methods and Materials

2.1. Site description

4   The study was conducted in the watershed of the Tsuzura River, a midstream tributary of the

5 Shimanto River basin in Kochi Prefecture, southern Japan (Fig. 2). The watershed is located at

6 33°10′N, 132°57′E, and ranges in elevation from 405 to 545 m. Shale makes up the bedrock.

7 The climate is temperate humid monsoon, and the mean annual precipitation at the Taisho

8 weather station (4.8 km northeast of the study site) was 2735 mm from 1979 to 2000.

9   We established a throughfall observation site on a mountainous slope at an elevation of

10 420 m in a plantation of Japanese cypress, ranging in age from 36–40 years old. The average

11 slope gradient around the site was 26.3°. At the site, the mean tree height was 15.1 m, the mean

12 first living branch height was 7.9 m, and the mean diameter at breast height (DBH) was 21.6 cm.

13 The canopy closure rate was 14.5%, calculated with CanopOn 2 software

14 (http://takenaka-akio.cool.ne.jp/etc/ canopon2/) from hemispherical photographs of the site.

15 There was no understory vegetation. Examination of the soil profile showed a small A_0 horizon

16 and an A horizon composed of clay loam soils that were exposed to the surface.

17   Additionally, an open site was established 600 m east of and 300 m lower than the

18 throughfall site to compare the characteristics of rainfall intensity with throughfall.

19

2.2. Data collection

2.2.1 Meteorological factors: Rainfall intensity and wind speed

Rainfall depth and intensity were measured using a 0.2-mm tipping bucket rain gauge (RC-10; Davis Instruments Corp., CA, USA); tip time was recorded at 0.5-s accuracy using a data logger (HOBO Event; Onset Computer Corp., MA, USA) at both the throughfall site and the open site. Observations were conducted from 1 July to 28 November 2005, during the rainy season in Japan. Table 1 presents rainfall characteristics for the entire observation period; over 151 days, we observed 19 rainfall events and 47 rainy days. The total throughfall was 835.4 mm. The greatest precipitation occurred in Period IV as a result of a typhoon event on 4–6 September, which yielded 357.6 mm of throughfall precipitation. Overall, throughfall rainfall intensity was collected without any missing data; however, rainfall intensity was not measured at the open site during the Period IV typhoon event.

Wind speed was measured every 5 min, at 2 m above the ground using a three-cup anemometer (AC750; Makino Applied Instruments Corp., Tokyo, Japan) equipped with a data logger (SQ1250; Grant Instruments, Ltd., Cambridgeshire, UK). The measuring point was along a skid trail on a landslide scar, 50 m from the throughfall site, where measurements of upslope and downslope winds received by the forest canopies were considered possible. Wind speed was measured during 15–29 July and 10 August–14 September 2005.

2.2.2 Raindrop size and velocity

Throughfall raindrops were measured during seven rainfall events from Periods I–IV, using

1 a laser drop-sizing gauge (LD gauge) as described by Nanko et al. (2006). The LD gauge

2 includes a paired laser transmitter and receiver (LX2-02; KEYENCE Corp., Osaka, Japan).

3 When a raindrop passes through the laser sheet, the output voltage from the receiver is reduced

4 in proportion to the intercepted area. Raindrop sizes were calculated from the relationship

5 between the interception rate and the output voltage. The reliability of drop sizing by the LD

6 gauge was confirmed by a calibration experiment using glass spheres and water drops.

7   Each falling raindrop was assumed to have an oblate spheroid shape, like that of raindrops

8 at near-terminal velocity (Beard, 1976), with a flat ratio determined using equations proposed

9 by Pruppacher and Pitter (1971):

10 $$\frac{b}{a} = 1 \qquad (D \leq 1 \text{ mm}) \qquad\qquad \text{(Eq. 1)}$$

11 $$\frac{b}{a} = 1.05 - 0.0655D \qquad (D > 1 \text{ mm}) \qquad\qquad \text{(Eq. 2)}$$

12 where a is the major axis of an oblate spheroid (mm), b is the minor axis of an oblate spheroid

13 (mm), and D is the equivalent spheroid diameter (mm) calculated from raindrop volume

14 assuming sphericity. Raindrop velocity (V: m s^{-1}) was calculated from LD gauge data as

15 $$V = \frac{b + L - d}{T} \qquad\qquad \text{(Eq. 3)}$$

16 where b is the minor axis of a raindrop oblate spheroid (mm = 10^{-3} m), L is the laser sheet width

17 (1 mm = 1×10^{-3} m), T is the intercepted time (ms = 10^{-3} s) measured by the LD gauge, and d is

18 the necessary distance to detect a raindrop (mm = 10^{-3} m), specifically the necessary intercept

19 distance to produce a voltage reduction of more than 0.05 V. The LD gauge does not log voltage

20 reduction values less than 0.05 V because of denoising.

9

1   It is possible that the drips were not oblate spheroid in shape because their velocity did not

2   reach the terminal velocity. Raindrops with diameters >2 mm must fall at least 9 m to accelerate

3   to terminal velocity in air at 1 hPa and 20°C (Wang and Pruppacher, 1977). Epema and Riezebos

4   (1984) observed that water drops alternated between prolate and oblate shapes for the first 2 m

5   of fall. They calculated the minimum fall height for water drops to have 10% deviation of the

6   axis ratio from the equilibrium shape for still air conditions; a fall height of 5 m is required for

7   drops over 3.5 mm in equivalent diameter, and 3 m is required for drops less than 3 mm in

8   equivalent diameter. Consequently, based on the 7.9-m height of the first living branch, the drips

9   in this study likely did not reach terminal velocity but had an oblate spheroid shape.

10   A new data-logging LD gauge was developed, *i.e.*, an LD gauge equipped with a data

11   logging system (OWL2pe; EME Systems, CA, USA) and an analog circuit developed by EME

12   Systems. Electric power was supplied by a 12-V DC battery connected to a solar panel. This

13   logging system is triggered by a wetness sensor that detects the initial throughfall drip and has

14   the capacity to measure 45,055 raindrops.

15   The LD gauge could use two kinds of logging devices: a PC or the logging system. The

16   logging system did not require electricity but had less memory and slower processing speed than

17   the PC-logging system used by Nanko et al. (2006). The logging system records primary

18   processed data of output voltage to calculate the drop size and velocity, minimum output voltage,

19   base output voltage, and intercepted time and time stamp as one drop passes through the laser

20   sheet. After a drop passes through, the system requires more than 10 ms to process, writing the

1   data into memory and preparing to log the next drop. Consequently the data logger has the

2   disadvantage of failing to count some drop(s) when raindrops continuously pass through the

3   laser sheet, particularly under conditions of higher rainfall intensity.

4   The performance of the LD gauge was evaluated using a raindrop capture ratio, as used by

5   Nanko et al. (2004); the ratio of the rainfall volume measured by the LD gauge was compared

6   with that measured by the tipping-bucket rain gauge. The rainfall volume measured by the LD

7   gauge was determined by calculating the cumulative total drop volume. Figure 3 presents the

8   raindrop capture ratio of the two logging devices. Under higher rainfall intensities, the PC

9   logger maintained a high raindrop capture ratio (around 1.0), but the logging system yielded a

10 reduced raindrop capture ratio. However, we confirmed that the DSDs simultaneously measured

11 by the devices were similar and the difference in the median volume diameter, D_{50}, was only

12 ±0.05 mm. This result showed that the logger system could determine the qualitative raindrop

13 size distribution, and the drop capture rate could be used to quantitatively manipulate raindrop

14 data.

15

16 *2.2.3 Raindrop indices controlling soil splash detachment*

17   Three raindrop indices were used in this study, the kinetic energy (KE: J m^{-2}), the

18 momentum (M: kg m s^{-1} m^{-2}), and the momentum multiplied by the drop diameter (MD: kg m s^{-1}

19 mm m^{-2}). Salles and Poesen (2000) showed that MD is the best raindrop index of soil splash

20 detachment. Each index is calculated using the raindrop size and velocity. The kinetic energy (e:

1 J) and the momentum (p: kg m s^{-1}) of a raindrop can be calculated using the following equations:

2 $$e = \frac{1}{2}mV^2 = \frac{1}{2}\rho \cdot \left(\frac{\pi}{6}D^3\right) \cdot V^2 \qquad \text{(Eq. 4)}$$

3 $$p = mV = 10^3 \cdot \rho \cdot \left(\frac{\pi}{6}D^3\right) \cdot V \qquad \text{(Eq. 5)}$$

4 where m is raindrop weight (g) and ρ is raindrop density (1×10^{-6} g m^{-3}). Thus, respective

5 raindrop indices over a definite period can be calculated using the following equations:

6 $$KE = \frac{1}{S} \cdot \sum_{i=1}^{n} e_i \qquad \text{(Eq. 6)}$$

7 $$M = \frac{1}{S} \cdot \sum_{i=1}^{n} p_i \qquad \text{(Eq. 7)}$$

8 $$MD = \frac{1}{S} \cdot \sum_{i=1}^{n} p_i D_i \qquad \text{(Eq. 8)}$$

9 where S is the LD gauge sampling area (800 mm^2 = 8×10^{-4} m^2) and n is the number of drops

10 over a definite period.

11 In this paper, we use different variables for the throughfall drop indices: 10-min data for KE,

12 M, and MD; the total amount; and the maximum values in a definite period (KE_{MAX}, M_{MAX}, and

13 MD_{MAX}). In the discussion, we use unit kinetic energy (KE_{mm}: J m^{-2} mm^{-1}), the kinetic energy

14 per unit area, and unit volume of precipitation to calculate throughfall kinetic energy using the

15 model.

16

17 *2.2.4 Soil splash detachment*

1   Soil splash detachment was measured using splash cups, as described by Morgan (1978). Figure

2   4 presents the splash cup design, which consisted of a hollow cylinder pushed into the ground so

3   that the top was flush with the soil surface, a circular catching tray, and a partition board

4   dividing the catching tray into upslope and downslope compartments. The tray partition was

5   designed to measure net downslope transport but was not used in this study. We evaluated only

6   soil splash detachment. The exposed soil area was 78.5 cm^2 (a circle, 10 cm in diameter).

7   Because raindrops have greater kinetic energy than open rainfall (Chapman, 1948; Nanko et al.,

8   2004) and precipitation and rainfall intensity at the field site were very high, the boundary wall

9   size was increased to a height of 20 cm and a diameter of 20 cm to prevent splash-in from

10 outside and splash-out from the cup. The cup slope (θ_2 in Fig. 4) was reduced to nearly 0° so as

11 to prevent rainfall from entering the exposed soil area. A total of 27 splash cups were set on the

12 forest floor. The pipe slope (θ_1 in Fig. 4) ranged from 9 to 39°, and the mean slope declination

13 was 26.3°. The slope length of the splash cup was so small that runoff effects could safely be

14 excluded (Torri and Poesen, 1992); hence, the observed effects must have depended on factors

15 intrinsic to the soil splash process or to changes in soil detachability.

16   All the soil particles that detached by splashing and caught in the catch tray during rainfall

17 events were collected after the events. The collected samples were dried at 105°C for 24 h in a

18 dry oven and then weighed in the laboratory. The organic matter content was also analyzed by

19 measuring the ignition loss after heating the samples at 450°C for 5 h.

20   Owing to a failure in the sampling design, the splash cup could catch not only soil detached

1 from the ground surface but also litter fall from the trees. During the observations, litter

2 collected in the splash cup, especially during typhoon events, and mixed with detached soil in

3 the catch tray. To investigate the relationship between the splash detachment and the raindrop

4 indices, the litter fall had to be removed. However, because it was difficult to remove only the

5 litter fall from the collected materials, we focused on only the mineral particles detached from

6 the ground surface. The mineral fraction of the collected materials was evaluated by subtracting

7 the weight of the organic fraction from that of the total collected material.

8 As explained by van Dijk et al. (2002b), there is an experimental bias in measuring the soil

9 splash detachment. The measured rates of soil splash detachment are only the apparent rates and

10 are specific to the geometry of the experimental device and the size distribution of the splashed

11 soil particles. The apparent soil splash rate m_R (g m^{-2})—calculated as the mass (g) of soil

12 splashed from a cup of radius R (m) divided by its surface area (m^2)—is related to the average

13 soil splash length Λ (m) and the actual detachment rate μ (g m^{-2}), expressed by the following

14 equation, called the fundamental splash distribution function:

15
$$m_R = \left[1 - \exp\left(-\frac{\pi}{2}\frac{R}{\Lambda}\right)\right]\frac{2}{\pi}\frac{\Lambda}{R}\mu \qquad\qquad (\text{Eq. 9})$$

16 Thus, measured soil splash detachment rates should underestimate the actual detachment rates

17 (van Dijk et al., 2002b; van Dijk et al., 2003; Leguédois et al., 2005). In this study, all the

18 experimental devices had the same geometry. The size distributions of the splashed soil particles

19 probably had important variations, but the only variability factor that could have acted on the

1   splash detachment measurements would have been the raindrop size. However, as shown by

2   Furbish et al. (2007), soil splash distances are not dependent on raindrop size. Thus,

3   device-related size bias was neglected in the present study.

4

5   ***3. Results***

6   ***3.1. Throughfall drops***

7   Figure 5 presents observation data for the rainfall event of 19–20 August 2005 taken over

8   10-min periods, illustrating temporal variation in mean wind speed (m s^{-1}), rainfall intensity

9   (mm 10-min^{-1}) at the open site and throughfall site, and contour plans of throughfall drops per

10   10-min interval. Open rainfall precipitation was 24.2 mm, and throughfall precipitation was

11   21.4 mm. Peak rainfall intensity was greater for throughfall than for open rainfall.

12   Throughfall drops were large, with a maximum drop size of 6.11 mm in diameter. Drops

13   exceeding 2 mm in diameter were observed even when the tipping-bucket rain gauge did not

14   measure the amount of throughfall. Large drops exceeding 4 mm in diameter were observed

15   when throughfall had intensities greater than 1 mm 10-min^{-1}. The generation of large drops for

16   Japanese cypress was less associated with open rainfall intensity (Nanko et al., 2006).

17   Figure 6 presents the DSD during the rainfall event described in Fig. 5. The DSD was based

18   on the volume ratio normalized by the total volume of raindrops, using 0.3-mm-diameter classes

19   and a minimum diameter of 0.5 mm. We assumed DSD values at the open site, for reference, and

20   cumulated DSDs every 10 min using open rainfall intensity and the model proposed by Marshall

1 and Palmer (1948). The assumed open rainfall had a unimodal DSD, with a mode about 1 mm in

2 diameter. Throughfall had a bimodal DSD; the first mode had a diameter of about 1 mm, and the

3 second of about 4 mm. The median volume diameter, D_{50}, was 1.18 mm for open rainfall and

4 2.00 mm for throughfall. The D_{50} of all observed throughfall drops was 1.99 mm. These values

5 are considered well bounded. The D_{50} of Japanese cypress plantations reported by Nanko et al.

6 (2006) ranged from 1.77 to 2.14 mm in windy or calm conditions.

7 Throughfall drop velocity was measured, and Fig. 7 presents the relationship between drop

8 diameters and velocities for all drops measured in this study using a contour plan. Solid lines

9 indicate the terminal velocity of drops calculated using the equation presented by van Dijk et al.

10 (2002a). Broken lines represent the assumed drop velocity when drops fell from a height of 8 m,

11 which was the value nearest to the height of the first living branch (7.9 m) in this study, as set out

12 by Laws (1941).

13 Drops with diameters smaller than 1 mm almost reached terminal velocity. These drops

14 included free throughfall and splashed water droplets (Nanko et al., 2006). Free throughfall

15 originally had terminal velocity. Splashed water droplets were so light that drops only required a

16 short fall height to gain terminal velocity. In contrast, drops with diameters >3 mm did not come

17 close to reaching terminal velocity. In total, 323 drops had diameters >3 mm, and 294 of these

18 drops (91% of the total) had less than 90% terminal velocity. These drops were almost entirely

19 composed of drips (Nanko et al., 2006), and the fall height was insufficient for drips to gain

20 terminal velocity. Raindrops with diameters >3 mm must fall at least 12 m to accelerate to

1   terminal velocity (Wang and Pruppacher, 1977).

2   Some drips had velocities slower than expected of a drop falling from the height of the first

3   living branch (broken line in Fig. 7). Drips were probably generated not only from leaves on

4   living branches but also from dead branches and areas adjacent to tree stems. Additionally, the

5   prolate shapes of some drips suggest that their velocities could have been underestimated

6   (Epema and Riezebos, 1984).

7

8   *3.2. Throughfall raindrop indices and soil splash detachment in forests*

9   Figure 8 presents the relationship between throughfall rainfall intensity and throughfall

10   raindrop indices, *KE*, *M*, and *MD*, based on a 10-min period dataset. Although throughfall

11   raindrops were measured during seven rainfall events under different meteorological conditions,

12   *KE* and *M* had a strong linearity with rainfall intensity (the coefficients of determination were

13   0.96 and 0.99, respectively), and *MD* was strongly correlated with rainfall intensity by the

14   power function (the coefficient of determination was 0.98). The following regression formulas

15   were obtained:

16   $KE = 16.4I$ (Eq. 10)

17   $M = 5.49I$ (Eq. 11)

18   $MD = 22.5I^{1.30}$ (Eq. 12)

19   where I is rainfall intensity (mm 10-min^{-1}). Throughfall-DSD fluctuated relative to open rainfall

20   intensity, wind speed, or both, but only a small fluctuation was observed in Japanese cypress

1 (Nanko et al., 2006). Accordingly, it appeared that throughfall raindrop indices at this study site

2 fluctuated only a little, independent of meteorological factors. Equations 10–12 were used to

3 estimate indices of total raindrop amounts for rainfall events with no raindrop measurements.

4 We calculated the raindrop indices using 10-min rainfall intensity measured using the

5 tipping-bucket rain gauge.

6   Figure 9 and part of Table 2 present temporal variations in throughfall precipitation

7 (mm day^{-1}); the total throughfall raindrop indices, KE (10^3 J m^{-2}), M (10^3 kg m s^{-1} m^{-2}), and MD

8 (10^3 kg m s^{-1} mm m^{-2}); and the soil splash detachment rate (g m^{-2}) over each observation period.

9 During the overall observation period, the total throughfall amounted to 835.4 mm in

10 precipitation, 13.7×10^3 J m^{-2} in KE, 4.58×10^3 kg m s^{-1} m^{-2} in M, and 20.6×10^3 kg m s^{-1}

11 mm m^{-2} in MD. The total soil splash detachment rates observed in each splash cup over the

12 entire period ranged from 312 to 7381 g m^{-2} (3214 g m^{-2} on average; $\sigma = 1437$ g m^{-2}). In each

13 period, the mean soil splash detachment rates ranged from 107–1034 g m^{-2}, showing a

14 maximum in Period IV. The soil splash detachment rates in Period I were almost as high as the

15 maximum shown in Period IV, which included the typhoon event, and declined thereafter. This

16 pattern was attributed to an initial increase in soil splash detachment rates due to the continued

17 saturation of the surface, followed by an exhaustion of available material that was detachable by

18 raindrop impact (Parsons et al., 1994; Wainwright et al., 2000).

19   Soil splash detachment was weakly correlated with the total-amount raindrop indices.

20 Period I had about 80% lower KE, M, and MD than did Period IV but only 8% smaller soil splash

1 detachment rates. Period II had similar KE and M values and 23% greater MD than Period V, but

2 the splash detachment rates in Period II were more than five times those in Period V. Figure 10

3 presents the relationship between the soil splash detachment rate (kg m^{-2}) and total KE (kJ m^{-2})

4 for each observation period. The soil splash detachment rates had weak linearity with total KE.

5 Table 3 presents Pearson's product-moment correlation coefficient and the two-sided p-values

6 for the rainfall erosivity indices and soil splash detachment rates. Soil splash detachment rates

7 and total KE had a correlation coefficient of 0.632. The soil detachment rates showed weak

8 linearity to two other raindrop indices (Table 3) and the other rainfall erosivity factor, EI_{30}

9 (Wischmeier and Smith, 1978).

10

11 **4. Discussion**

12 **4.1. Characteristics of throughfall kinetic energy: Comparison between observed and**

13 **estimated values**

14   We investigated the characteristics of the kinetic energy of throughfall by comparing the

15 data from this study with estimates calculated using a previous model (Brandt, 1990). The

16 Brandt model has been widely used to calculate throughfall-KE; for example, it is applied in the

17 Morgan–Morgan–Finney (Morgan et al., 1984, revised by Morgan, 2001) and EUROSEM

18 models (Morgan et al., 1998). The Brandt model calculates unit kinetic energy (KE_{mm}: J m^{-2}

19 mm^{-1}), but 10-min-based KE was used for the comparison because Salles et al. (2002) concluded

20 that time-specific rain kinetic energy was more appropriate than volume-specific rain kinetic

19

1   energy when using DSD data collected by an automatic measuring device. The 10-min KE was

2   calculated using the following equation:

3    $KE = KE_{mm} \cdot I$

4   Open-KE_{mm} was calculated using the following equation:

5    $KE_{mm}[OP] = 8.95 + 8.44 \log_{10} I_{1h}$ (Eq. 13)

6   where $[OP]$ represents open rainfall, and I_{1h} is hourly rainfall intensity (mm h^{-1}).

7   Throughfall-KE_{mm} was calculated using the following equations:

8    $KE_{mm}[TH] = p \cdot KE_{mm}[OP] + (1-p) \cdot KE_{mm}[DR]$ (Eq. 14)

9    $KE_{mm}[DR] = c\sqrt{PH} - d$ (Eq. 15)

10    $PH = H_{bottom} + \dfrac{1}{(LAI+1)}\left(H_{top} - H_{bottom}\right)$ (Eq. 16)

11   where $[TH]$ and $[DR]$ represent throughfall and leafdrip, respectively. PH is the plant height

12   index, H_{bottom} is the height of the first branch, and H_{top} is the tree height. For p, the free

13   throughfall ratio, we used 0.145 because of the canopy openness. LAI is leaf area index, the ratio

14   of the total upper leaf surface of a tree divided by the surface area of the land on which the tree

15   grows; we used a value of 4. For the constants c and d, fixed numbers determined by the mean

16   volume drop diameter of leafdrips, we chose 14.5 and 4.99, respectively, based on Brandt

17   (1990), because the second mode of the throughfall DSD was around 4 mm in diameter (Fig. 6).

18   Figure 11 presents the relationship between KE and rainfall intensity. The plots indicate

19   observed throughfall-KE. Two lines indicate KE estimated by the Brandt model: the solid line

1 represents open-*KE*, and the broken line represents throughfall-*KE*. Observed throughfall-*KE*

2 was greater than estimated open-*KE* because throughfall had larger drops, which may have

3 consisted of drips. In contrast, observed throughfall-*KE* was much lower than estimates. The

4 slope of the estimated throughfall-*KE* was approximately 35 J m^{-2} mm^{-1}, about two times the

5 measured throughfall-*KE*. The Brandt model probably overestimated throughfall-*KE* for two

6 reasons. First, some drips had a lower velocity than expected for a drop falling from the height

7 of the first living branch (broken line in Fig. 7). It is possible that drips were not only generated

8 from leaves on living branches, but also from dead branches and areas adjacent to the tree stem.

9 Therefore, throughfall drop velocity should not be determined based on the first living branch

10 height alone.

11   Second, the Brandt model separates throughfall into two components: free throughfall, i.e.,

12 raindrops passing through a canopy without striking the vegetation, and leafdrips. A similar

13 separation is applied in interception process models such as those by Rutter et al. (1971), Gash

14 (1979), and Calder (1996). However, Nanko et al. (2006) suggested that throughfall also

15 consisted of a water splash component: water droplets produced by the impact of raindrops on a

16 canopy and spattering water caused by wind vibration in a canopy. Splash water droplets have

17 much less kinetic energy than drips. Accordingly, the Brandt model may overestimate

18 throughfall-*KE* because it considers all throughfall (except free throughfall) to be leafdrips.

19 More detailed actual measurements are needed to construct a model to calculate throughfall

20 kinetic energy.

1   Brandt (1990) also presented a model to estimate throughfall momentum. Another

2   comparison between the measured and estimated momentum values produced results similar to

3   those for kinetic energy.

4

5   *4.2. Characteristics of soil splash detachment in forests*

6   Experimental studies have revealed that the soil splash detachment rate depends on the total

7   kinetic energy of rain (Mihara, 1951; Free, 1960; Quansah, 1981; Poesen, 1985; Al-Durrah and

8   Bradford, 1988; Morgan et al., 1998). In soil erosion process models (Morgan et al., 1998;

9   Morgan, 2001), soil splash detachment is calculated at 1.0 power of kinetic energy. However,

10   the present study conducted in a forest, found a weak correlation between the soil splash

11   detachment rate and kinetic energy for each observation period (Fig. 10 and Table 3). Other

12   indices, the momentum, the momentum multiplied by the drop diameter, and EI_{30}, also weakly

13   correlated with the soil splash detachment rate (Table 3).

14   The soil splash detachment rate also depends on rainfall intensity or instantaneous drop

15   impact as well as the total amount of rainfall, or other raindrop indices. We estimated the effect

16   of instantaneous raindrop impact, expressed as the maximum value of raindrop indices during

17   each observation period using various time scales. Table 2 presents the maximum rainfall

18   intensity (I_{MAX}: mm h^{-1}) and raindrop indices KE_{MAX} (J m^{-2} h^{-1}), M_{MAX} (kg m s^{-1} m^{-2} h^{-1}), and

19   MD_{MAX} (kg m s^{-1} mm m^{-2} h^{-1}) over each time scale: total, 24-h, 3-h, 1-h, 30-min, and 10-min.

20   Each value was converted to a 1-h time unit.

1   Figure 12 presents the relationship between the soil splash detachment rate and two

2 raindrop indices, KE_{MAX} and MD_{MAX}, over each time scale. KE and M were calculated from

3 rainfall intensity (I) using the linear regression equations (Eqs. 10 and 11) so that the

4 relationship between the soil detachment rates and I_{MAX} or M_{MAX} was the same as that for KE_{MAX}

5 (the upper part of Fig. 12). The soil splash detachment rate had a stronger correlation with

6 KE_{MAX} or MD_{MAX} than with total KE or total MD (Table 10). The correlation with the maximum

7 value was particularly strong on short time scales (1 h or less), with a correlation coefficient

8 exceeding 0.89 (p < 0.02). The soil splash detachment rate was most strongly correlated with the

9 1-h maximum value; the correlation coefficient was 0.954 (p = 0.003) for KE_{MAX} and 0.995

10 (p = 0.000) for MD_{MAX} (Table 3). MD showed relatively higher correlation with the soil splash

11 detachment rate than with other raindrop indices. We obtained the following regression

12 formulas using the 1-h maximum value of throughfall intensity or throughfall drop indices:

13     $D = 84.4 I_{MAX} - 566.9$ (Eq. 17)

14     $D = 5.14 KE_{MAX} - 566.9$ (Eq. 18)

15     $D = 15.4 M_{MAX} - 566.9$ (Eq. 19)

16     $D = 2.11 MD_{MAX} - 370.1$ (Eq. 20)

17   These results indicate that continuous and concentrative raindrop impacts over a short

18 period of time cause soil splash detachment on the forest floor. The development of a physically

19 based model of soil splash detachment on the forest floor will require the estimation of the effect

20 of temporal variations in rainfall intensity and in raindrop indices of soil splash detachment.

1

Conclusions

2

3   To study and model the interrill erosion process in an unmanaged Japanese cypress

4 (*Chamaecyparis obtusa*) plantation, throughfall raindrop indices and soil splash detachment

5 rates were quantified. We observed throughfall drop sizes and velocities and soil splash

6 detachment in the field for over five months in 2005, during six observation periods.

7 Throughfall drops were large, with a maximum drop size of 6.11 mm in diameter. Observed

8 throughfall drops had median volume diameters well bounded by measurements from other

9 Japanese cypress plantations: 1.99 mm over the entire observation period. Drops smaller than

10 1 mm in diameter, including free throughfall drops and splashed water droplets, reached

11 near-terminal velocity. In contrast, drops exceeding 3 mm in diameter, almost all of which were

12 drips, did not come close to reaching terminal velocity: 91% of the total drops with diameters

13 >3 mm had <90% terminal velocity. The fall height was insufficient for drips to gain terminal

14 velocity.

15   As raindrop indices of soil splash detachment, the kinetic energy (*KE*), the momentum (*M*),

16 and the momentum multiplied by the drop diameter (*MD*) of throughfall were calculated from

17 the diameters and velocities of drops. The observed throughfall raindrop indices had a strong

18 correlation with throughfall rainfall intensity, even though they were observed over seven

19 rainfall events with different meteorological conditions. *KE* and *M* were calculated from linear

20 regression functions, and *MD* was calculated from a power regression function with throughfall

1   rainfall intensity. The observed *KE* and *M* were lower than the values estimated by the Brandt

2   model (1990). The Brandt model overestimates throughfall *KE* and *M*. First, the observed drops

3   had lower velocity than expected given the first living branch height. Drips could have been

4   generated from leaves on living branches as well as dead branches and areas adjacent to the tree

5   stem. Second, the Brandt model considers all throughfall (except free throughfall) to be

6   leafdrips and does not include the water splash component (Nanko et al., 2006) of throughfall.

7   The water splash component had much lower *KE* and *M* values than did the leafdrips.

8   The soil splash detachment rate in forests was weakly correlated with the total-amount

9   raindrop indices but strongly correlated with the maximum value of raindrop indices over short

10   time scales, such as 1 h, for each raindrop index. This result indicates that continuous and

11   concentrative raindrop impacts over a short period of time cause soil splash detachment on the

12   forest floor. Our results indicate that the development of a physically based model of soil splash

13   detachment on the forest floor requires the estimation of the effects of temporal variations in

14   rainfall intensity and raindrop indices of soil splash detachment.

15

16 *Acknowledgments*

1   modeling studies on the effect of forest devastation on flooding and environmental issues."

2

1

2 ***References***

3 Akenaga, H., Shibamoto, T., 1933. Effect of soil elements in cypress forest plantations in the

4   Owase region. Journal of Japanese Forestry Society, 15: 19–26 (in Japanese).

5 Al-Durrah, M.M., Bradford, J.M., 1982. Parameters for describing soil detachment due to single

6   waterdrop impact. Soil Science Society of America Journal, 46: 836–840.

7 Beard, K.V., 1976. Terminal velocity and shape of cloud and precipitation drops aloft. Journal of

8   Atmospheric Sciences, 33: 851–864.

9 Brandt, J., 1989. The size distribution of throughfall drops under vegetation canopies. Catena,

10   16: 507–524.

11 Brandt, J., 1990. Simulation of the size distribution and erosivity of raindrops and throughfall

12   drops. Earth Surface Processes and Landforms, 15: 687–698.

13 Calder, I.R., Hall, R.L., Prasannab, K.T., 1993. Hydrological impact of Eucalyptus plantation in

14   India. Journal of Hydrology, 150: 635–648.

15 Calder, I.R., 1996. Dependence of rainfall interception on drop size 1: further development of

16   the stochastic model. Journal of Hydrology, 185: 363–378.

17 Calder, I.R., 2001. Canopy processes: implications for transpiration, interception and splash

18   induced erosion, ultimately for forest management and water resources. Plant Ecology, 153:

19   203–214.

20 Chapman, G., 1948. Size of raindrops and their striking force at the soil surface in a red pine

1 plantation. Transactions of American Geophysical Union, 29: 664–670.

2 Ellison, W.D., 1944. Studies of raindrop erosion. Agricultural Engineering, 25: 131–136.

3 Epema, G.F., Riezebos, H.T., 1984. Drop Shape and erosivity part 1: experimental set up, theory,

4 and measurements of drop shape. Earth Surface Processes and Landforms, 9: 567–572.

5 Free, G.R., 1960. Erosion characteristics of rainfall. Transactions of the American Society of

6 Agricultural Engineers, 41: 447–449, 455.

7 Furbish, D.J., Hamner, K.K., Schmeeckle, M., Borosund, M.N., Mudd, S.M., 2007. Rain splash

8 of dry sand revealed by high-speed imaging and sticky paper splash targets. Journal of

9 Geophysical Research–Earth Surface, 112: F01001.

10 Gash, J.H.C., 1979. An analytical model of rainfall interception by forests. Quarterly Journal of

11 Royal Meteorological Society, 105: 43–55.

12 Govers, G., 1991. Spatial and temporal variations in splash detachment: a field study. Catena

13 Supplement 20: 15–24.

14 Gunn, R., Kinzer, G.D., 1949. The terminal velocity of fall for water droplets in stagnant air.

15 Journal of Meteorology, 6: 243–248.

16 Hanson, D.L., Steenhuis, T.S. Walter, M.F., Boll, J., 2004. Effect of soil degradation and

17 management practices on the surface water dynamics in the Talgua River Watershed in

18 Honduras. Land Degradation and Development, 15: 367–381.

19 Hattori, S., Abe, T., Kobayashi, C., Tamai, K., 1992. Effect of forest floor coverage on reduction

20 of soil erosion in hinoki pkantations. Bulletin of the Forestry and Forest Products Research

1   Institute, 362: 1–34 (in Japanese with an English summary).

2   Kawana, A., Takahara, S., Matsunaga, E., Kubo, I., Hirayama, H., Aonuma, K., 1963. Studies

3   on protection of forest soil in Japanese cypress stands at Owase (I): Experiment on protection

4   of forest soil loss in cypress plantations. Transactions of Annual Meeting Japanese Forestry

5   Society, 74: 126–129 (in Japanese).

6   Kinnel, P.I.A., 2005. Raindrop-impact-induced erosion processes and prediction: a review.

7   Hydrological Processes, 19: 2815–2844.

8   Kiyono, Y., 1990. Dynamics and control of understories in *Chamaecyparis obtusa* plantations.

9   Bulletin of the Forestry and Forest Products Research Institute, 359: 1–122 (in Japanese with

10   an English summary).

11   Laws, J.O., 1941. Measurements of the fall-velocity of water-drops and raindrops. Transactions

12   of American Geophysical Union, 22: 709–721.

13   Leguédois, S., Planchon, O., Legout, C., Bissonnais, Y.L., 2005. Splash projection distance for

14   aggregated soils: theory and experiment. Soil Science Society of America Journal, 69:

15   30–37.

16   Marshall, J.S., Palmer, M.W., 1948. The distribution of raindrops with size. Journal of

17   Meteorology, 5: 165–166.

18   Mihara, Y., 1951. Raindrops and soil erosion. Bulletin of the National Institute of Agricultural

19   Sciences, A-1:1–59 (in Japanese with an English summary).

20   Miura, S., Hirai, K., Yamada, T., 2002. Transport rates of surface materials on steep forested

1   slopes induced by raindrop splash erosion. Journal of Forest Research, 7: 201–211.

2   Morgan, R.P.C., 1978. Field studies of rainsplash erosion. Earth Surface Processes and

3   Landforms, 3: 295–299.

4   Morgan, R.P.C., 2001. A simple approach to soil loss prediction: A revised

5   Morgan-Morgan-Finney model. Catena, 44: 305–322.

6   Morgan, R.P.C., Morgan D.D.V., Finney, H.J., 1984. A predictive model for the assessment of

7   erosion risk. Journal of Agricultural Engineering Research, 30: 245–253.

8   Morgan, R.P.C, Quinton, J.N., Smith, R.E., Govers, G., Poesen, J.W.A., Auerswald, K., Chisci,

9   G., Torri, D., Styczen, M.E., 1998. The European Soil Erosion Model (EUROSEM): A

10   dynamic approach for predicting sediment transport from fields and small catchments. Earth

11   Surface Processes and Landforms, 23: 527–544.

12   Mosley, M.P., 1982. The effect of a New Zealand beech forest canopy on the kinetic energy of

13   water drops and on surface erosion. Earth Surface Processes and Landforms, 7: 103–107.

14   Nanko, K., Hotta, N., Suzuki, M., 2004. Assessing raindrop impact energy at the forest floor in

15   a mature Japanese cypress plantation using continuous raindrop-sizing instruments. Journal

16   of Forest Research, 9: 157–164.

17   Nanko, K., Hotta, N., Suzuki, M., 2006. Evaluating the influence of canopy species and

18   meteorological factors on throughfall drop size distribution. Journal of Hydrology, 329:

19   422–431.

20   Park, S.W., Mitchell, J.K., Bubenzer, G.D., 1983. Rainfall characteristics and their relation to

1   splash erosion. Transactions of the ASAE, 26: 795–804.

2   Parsons, A. J., Abrahams, A. D., Wainwright, J., 1994. Rainsplash and erosion rates in an

3   interrill area on semi-arid grassland, southern Arizona. Catena, 22: 215–226.

4   Poesen, J., 1985. An improved splash transport model. Zeitschrift für Geomorphologie 29:

5   193–211.

6   Pruppacher, H.R., Pitter, R.L., 1971. A semi-empirical determination of the shape of cloud and

7   raindrops. Journal of Atmospheric Sciences, 28: 86–94.

8   Quansah, C., 1981. The effect of soil type, slope, rain intensity and their interaction on splash

9   detachment and transport. Journal of Soil Science, 32: 215–224.

10   Riezebos, H.T., Epema, G.F., 1985. Drop shape and erosivity part II: splash detachment,

11   transport and erosivity indices. Earth Surface Processes and Landforms, 10: 69–74.

12   Rose, C.W., 1960. Soil detachment caused by rainfall. Soil Science, 89: 28–35.

13   Rutter, A.J., Kershaw, K.A., Robins, P.C., Morton, A.J., 1971. A predictive model of rainfall

14   interception in forests: Derivation of the model from observations in a plantation of Corsican

15   pine. Agricultural Meteorology, 9: 367–384.

16   Sakai., M., Inoue, K., 1988. Effect of raindrops on the breakdown of cypress litter into small

17   pieces. Transactions of Japanese Forestry Society Kansai Branch Conference, 39: 43–46 (in

18   Japanese).

19   Salles, C., Poesen, J., 2000. Rain properties controlling soil splash detachment. Hydrological

20   Processes, 14: 271–282.

1 Salles, C., Poesen, J., Sempere-Torres, D., 2002. Kinetic energy of rain and its functional

2   relationship with intensity. Journal of Hydrology, 257: 256–270.

3 Terry, J.P., 1996. Erosion pavement formation and slope process interactions in commercial

4   forest plantations, northern Portugal. Zeitschrift fur Geomorphologie, 40: 97–115.

5 Torri, D., Poesen, J., 1992. The effect of soil surface slope on raindrop detachment. Catena, 19:

6   561–578.

7 Tsukamoto, Y., 1966. Raindrops under forest canopies and splash erosion. Bulletin of

8   Experimental Forest of Tokyo University of Agriculture and Technology, 5: 65–77 (in

9   Japanese with an English summary).

10 Tsukamoto, J., 1991. Downhill movement of litter and its implication for ecological studies in

11   three types of forest in Japan. Ecological Research, 9: 333–345.

12 Tsujimura, M., Onda, Y., Harada, D., 2006. The role of Horton overland flow in rainfall-runoff

13   process in an unchanneled catchment covered by unmanaged Hinoki plantation. Journal of

14   Japan Society of Hydrology and Water Resources, 19: 17–24. (in Japanese with an English

15   summary)

16 van Dijk, A.I.J.M., Bruijnzeel, L.A., Rosewell, C.J., 2002a. Rainfall intensity-kinetic energy

17   relationships: a critical literature appraisal. Journal of Hydrology, 261: 1–23.

18 van Dijk, A.I.J.M., Meesters, A.G.C.A., Bruijnzeel, L.A., 2002b. Exponential distribution

19   theory and the interpretation of splash detachment and transport experiments. Soil Science

20   Society of America Journal, 66: 1466–1474.

1   van Dijk, A.I.J.M., Bruijnzeel, L.A., Wiegman, S.E., 2003. Measurements of rain splash on

2   bench terraces in a humid tropical steepland environment. Hydrological Processes, 17:

3   513–535.

4   Vis, M., 1986. Interception, drop size distributions and rainfall kinetic energy in four Colombian

5   forest ecosystems. Earth Surface Processes and Landforms, 11: 591–603.

6   Wainwright, J., Parsons, A.J., Abrahams, A.D., 2000. Plot-scale studies of vegetation, overland

7   flow and erosion interactions: case studies from Arizona and New Mexico. Hydrological

8   Processes, 14: 2921–2943.

9   Wang, P.K., Pruppacher, H.R., 1977. Acceleration to terminal velocity of clouds and raindrops.

10   Journal of Applied Meteorology, 16: 275–280.

11 Wischmeier, W.H., Smith, D.D., 1978. Predicting rainfall erosion losses. A Guide to

12   Conservation Planning, Agricultural Handbook, vol. 537. US Department of Agriculture,

13   Washington, DC.

14 Yukawa, N., Onda, Y., 1995. The influence of understories on the infiltration capacities of

15   Chamaecyparis obtusa plantations (1) Experimental results using a mist type rainfall

16   simulator. Journal of Japan Forestry Society, 77: 224–231 (in Japanese with an English

17   summary).

18 Zhou, G., Wei, X., Yan, J., 2002. Impacts of eucalyptus (*Eucalyptus exerta*) plantation on

19   sediment yield in Guangdong Province, Southern China: A kinetic energy approach. Catena,

20   49: 231–251.

21

1 *Figure Captions*

2 Fig. 1   A Japanese cypress plantation with little surface cover, no undergrowth, and little litter.

3 Fig. 2   Study site location.

4 Fig. 3   Raindrop capture ratio: (a) data gathered by Nanko et al. (2006) using a PC-logging

5   system; and (b) data gathered during the present study using the logging system.

6 Fig. 4   Design of a splash cup.

7 Fig. 5   Temporal variations in meteorological factors and number of throughfall drops for

8   rainfall events over 10-min periods from 19–20 August 2005. Drop diameter is

9   presented both as a plot diagram and a contour plan using 0.3-mm diameter classes and

10   a minimum diameter of 0.5 mm.

11 Fig. 6 Drop size distribution (DSD) of throughfall and open rainfall during a rainfall event

12   from 19–20 August 2005, using 0.3-mm diameter classes and a minimum diameter of

13   0.5 mm. Throughfall DSD was observed, and open DSD was calculated. Each DSD was

14   normalized using the respective water volume.

15 Fig. 7 The relationship of drop velocity to drop diameter of whole observed throughfall drops

16   presented as a plot diagram (top) and a contour plan (bottom). Solid lines indicate

17   raindrop terminal velocity calculated using the method set out by van Dijk et al.

18   (2002a). Broken lines indicate the assumed drop velocity when drops fell from a height

19   of 8 m, which was the value nearest to the height of the first living branch at the site, as

1   set out by Laws (1941).

2   Fig. 8   The relationship between throughfall kinetic energy and rainfall intensity of

3   throughfall over 10-min periods ($n = 376$). The solid line represents the regression line

4   ($R^2 = 0.97$).

5   Fig. 9   Temporal variations in throughfall precipitation, kinetic energy, and splash detachment

6   rate during each observation period.

7   Fig. 10   The relationship between splash detachment rate and throughfall kinetic energy (KE)

8   during each observation period.

9   Fig. 11   Relationship of unit kinetic energy, KE_{mm}, to rainfall intensity over 10-min periods

10   ($n = 376$). Lines indicate the estimated KE_{mm} calculated using the Brandt model (1990).

11   Fig. 12   Relationship of splash detachment rate to maximum throughfall kinetic energy, KE_{MAX},

12   over various time scales.

13

Figure 1.

Figure 2.

Tsuzura-river watershed N 33° 10´, E 132° 57´

Study area

10 km

Tokyo

Osaka

Kochi Pref.

500 km

Figure 3.

Figure 4.

upslope

downslope

20 cm

20 cm

10 cm

cup slope: θ_2

Pipe slope: θ_1

weep hole
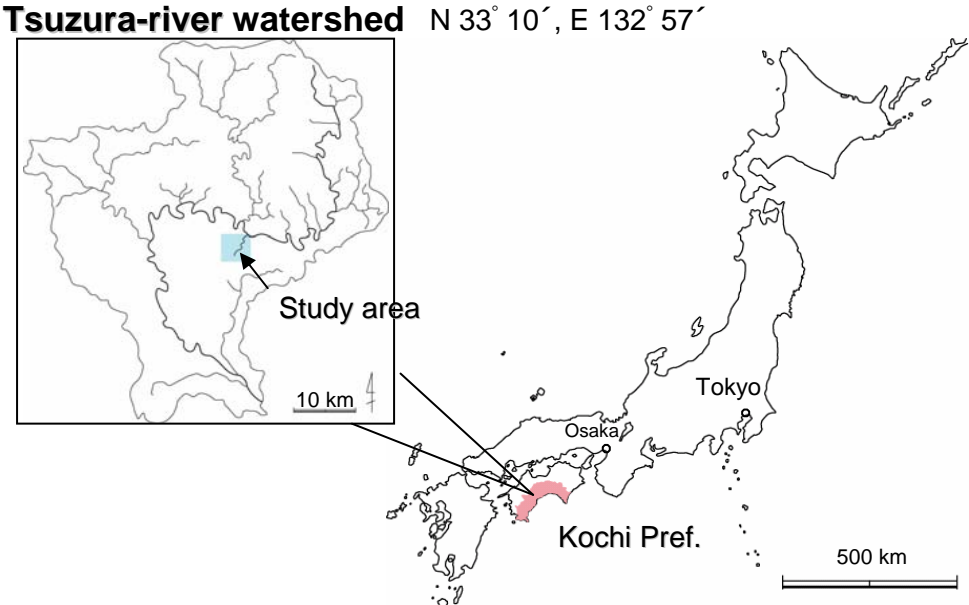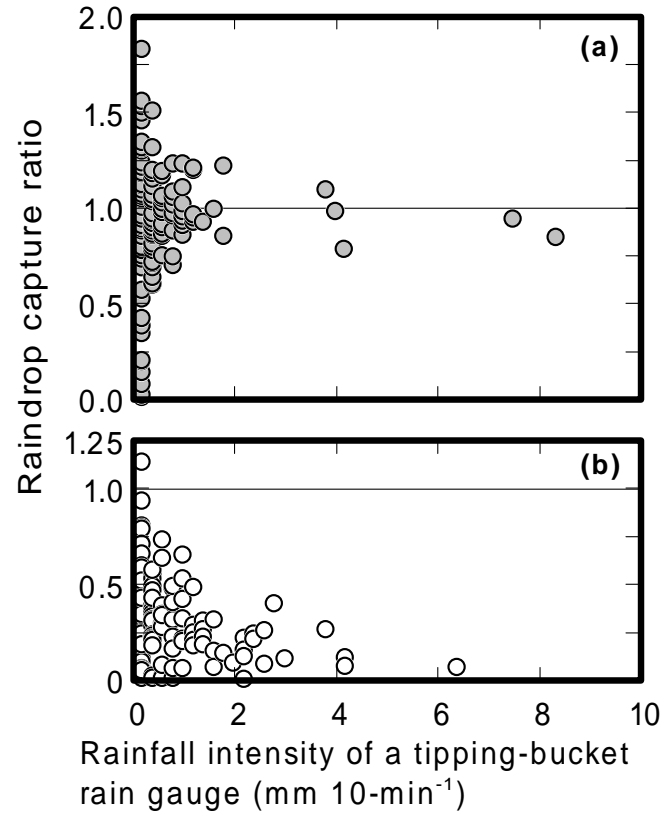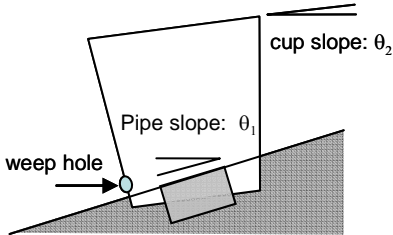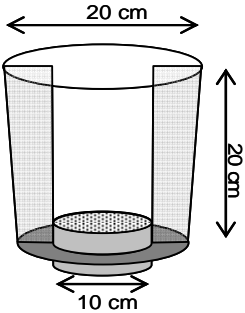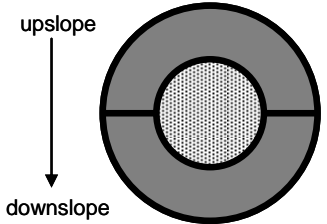
Figure 5.

Event 050819-20
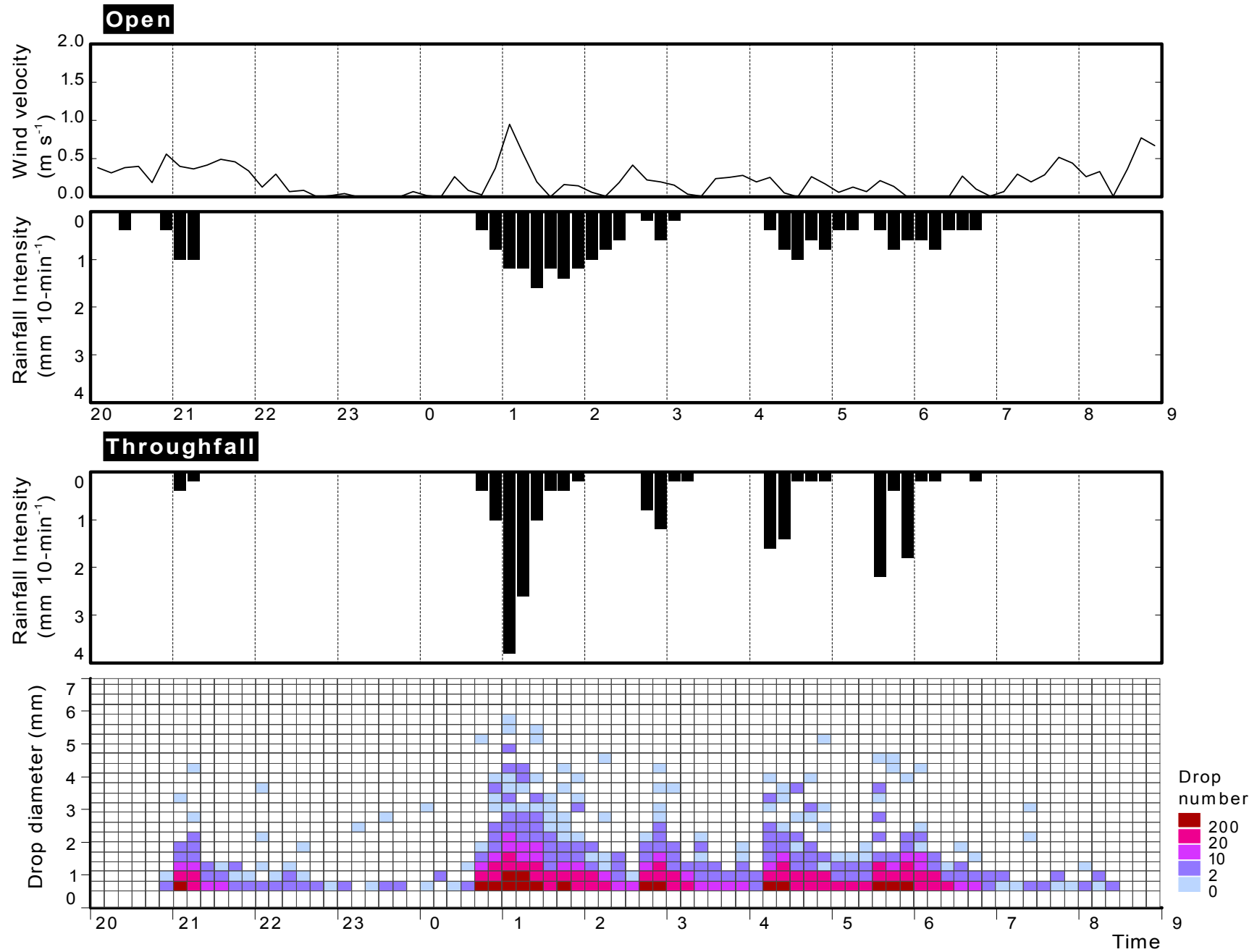
Figure 6.
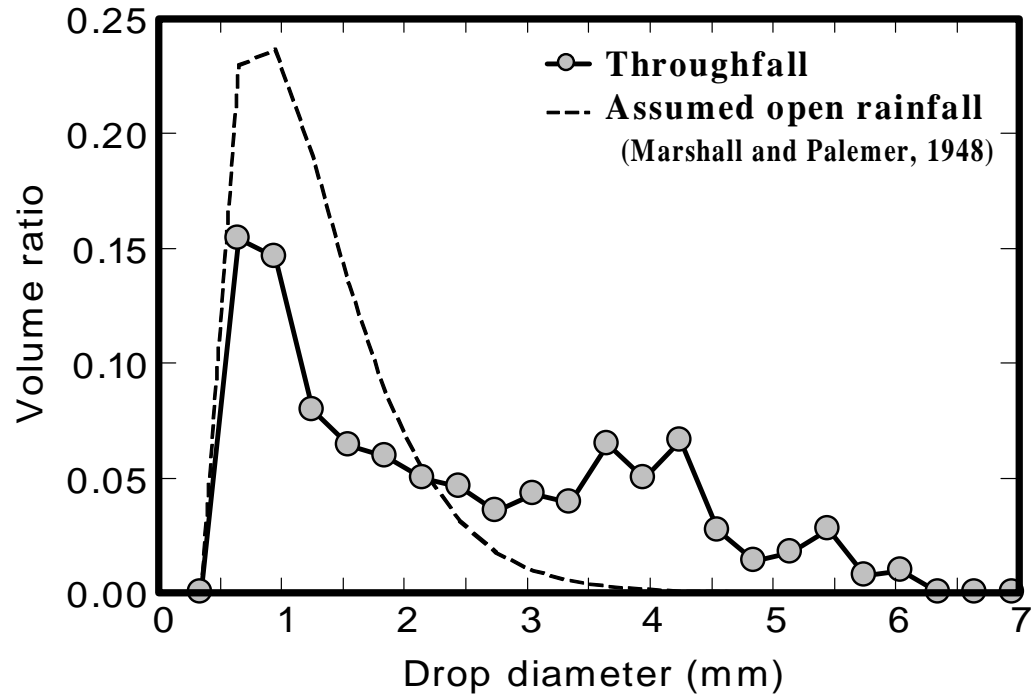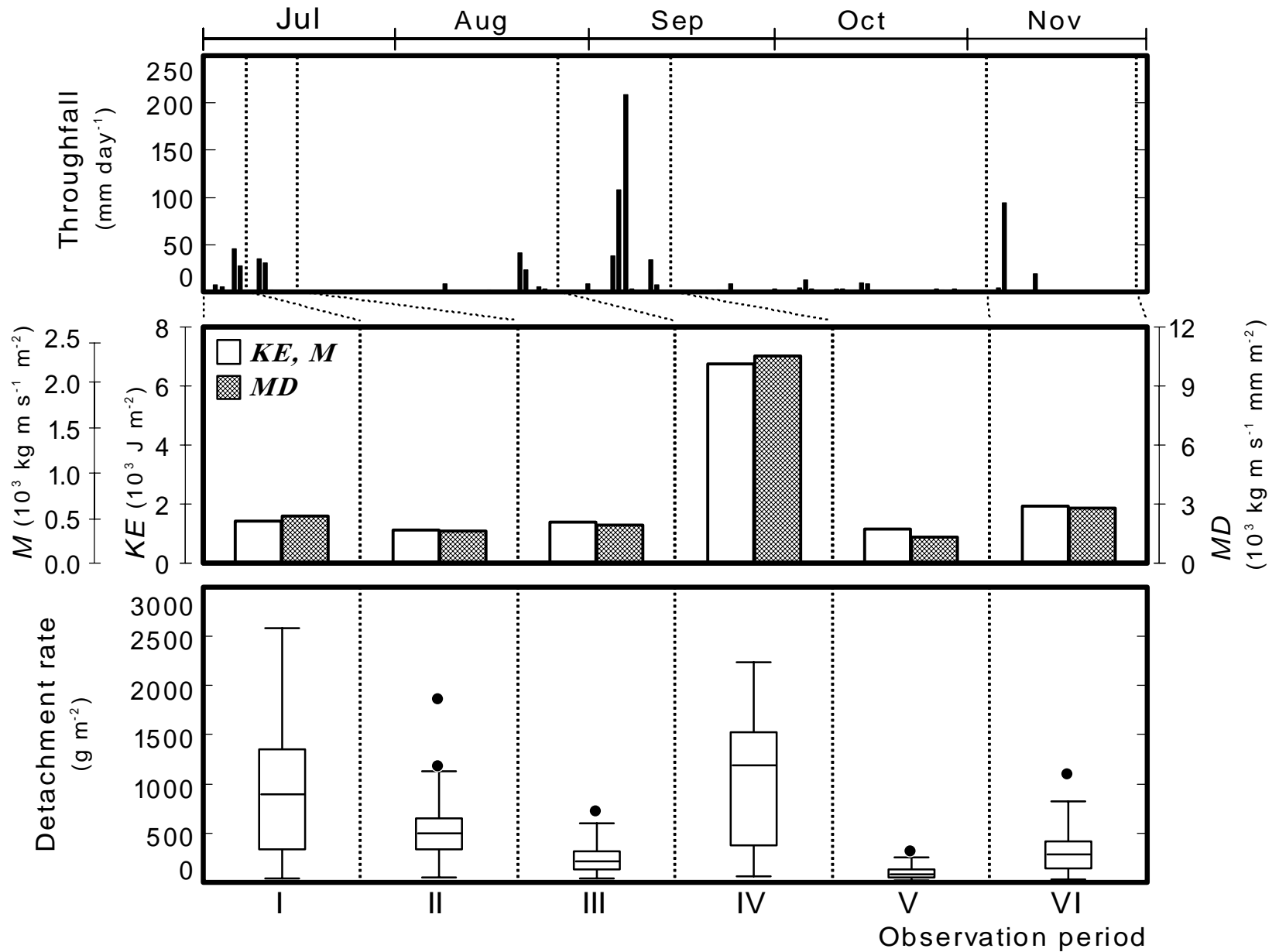
Figure 7.
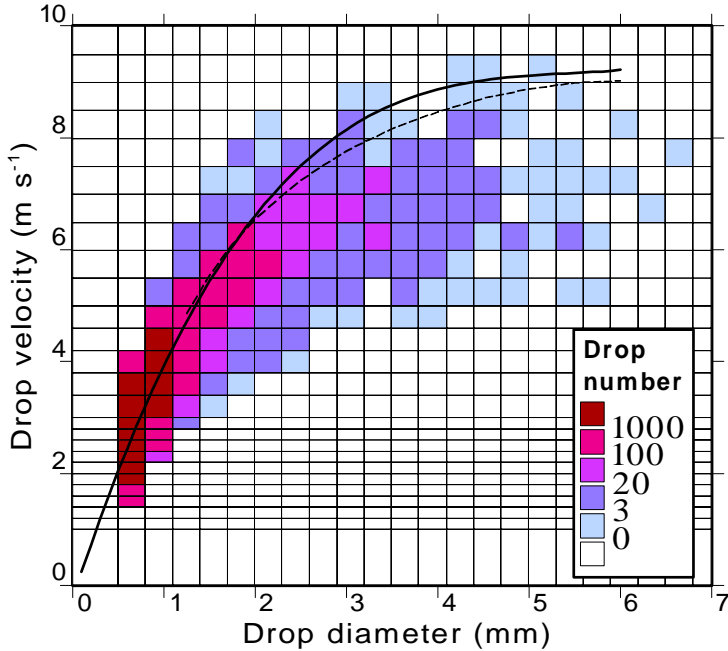
Figure 8.
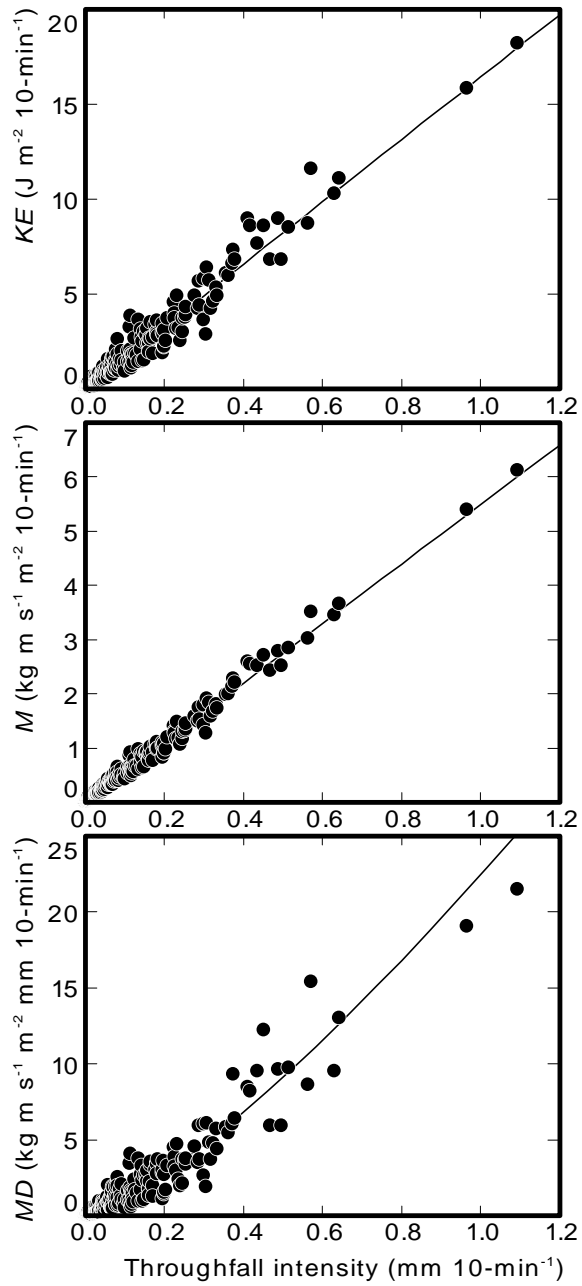
Figure 9.

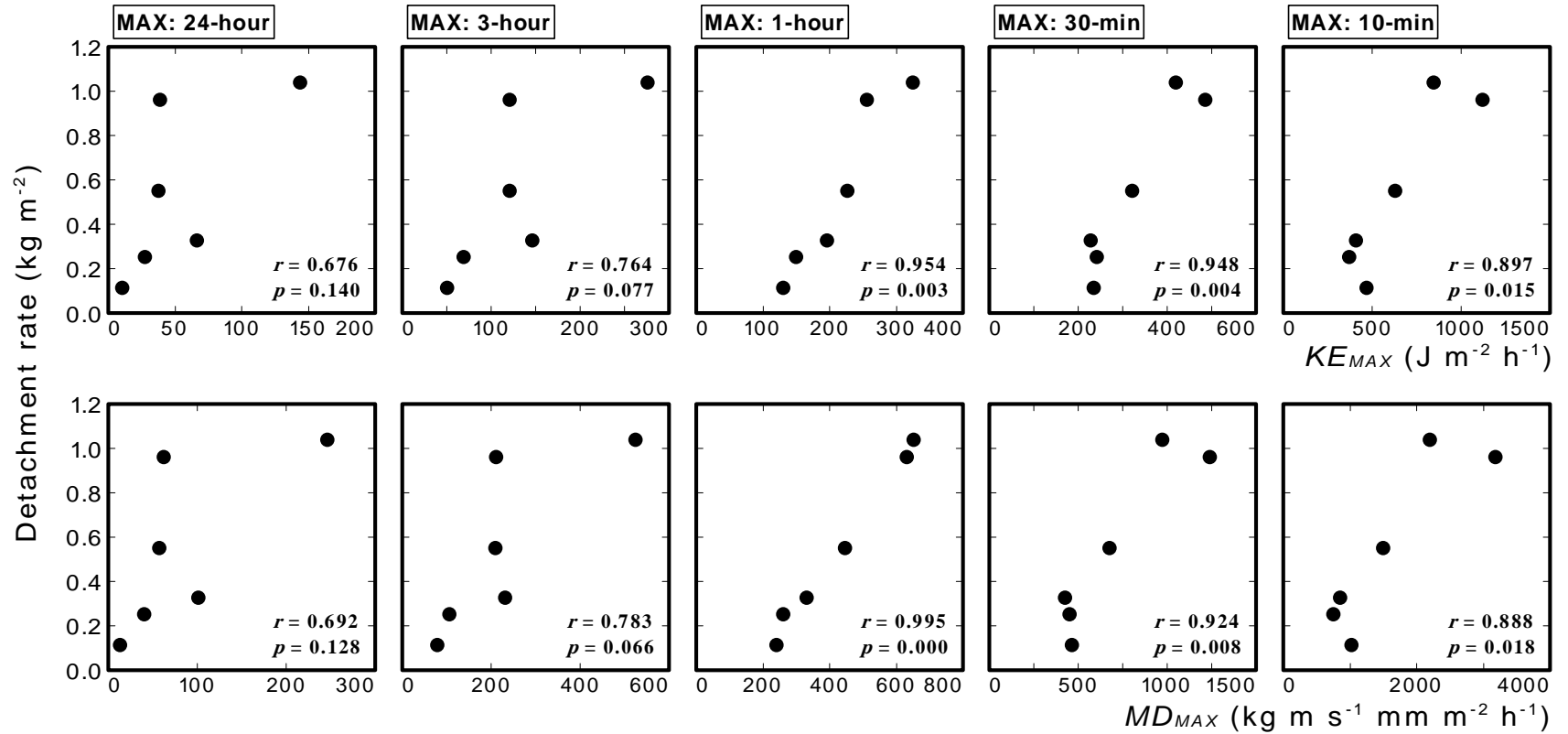**Figure 10.**
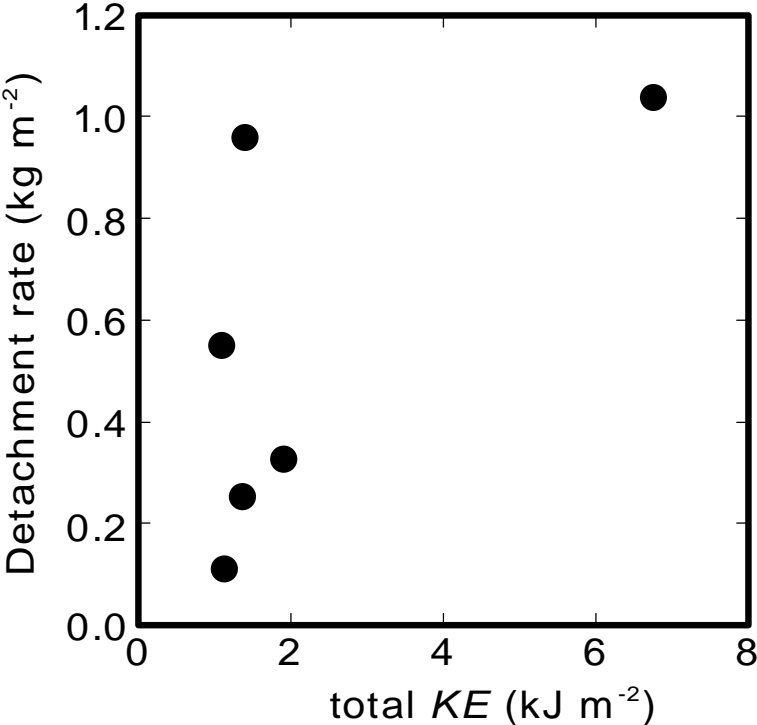
Figure 11.
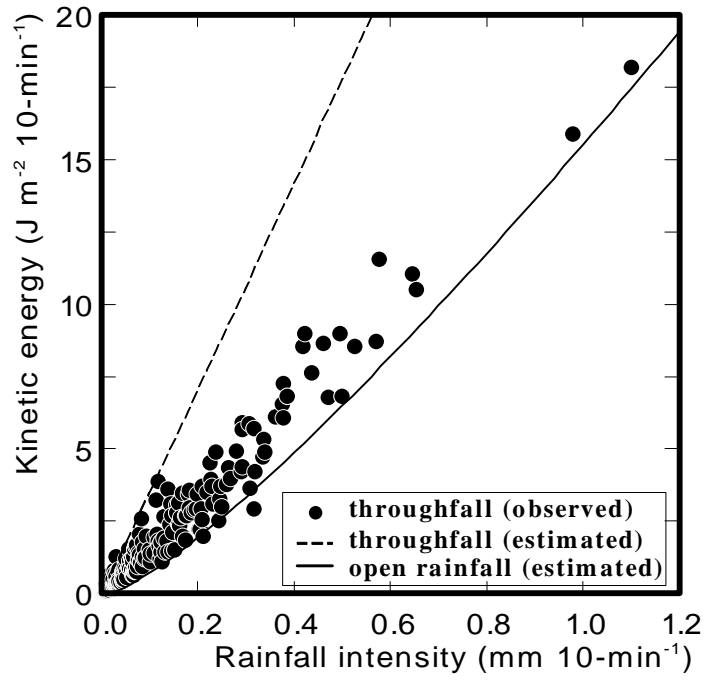
Figure 12.

Table 1. Rainfall characteristics of the six observation periods.

Period	I	II	III	IV	V	VI	Overall
Date in 2005	1 Jul – 7 Jul	8 Jul– 15 Jul	16 Jul– 26 Aug	27 Aug– 13 Sep	14 Sep– 3 Nov	4 Nov– 28 Nov	
Number of days	7	8	42	18	51	25	151
Number of rainy days	4	4	8	9	18	4	47
Number of storms	2	1	4	3	7	2	19
Max. rainfall in event mm	73.2	68.0	64.8	357.6	20.0	98.0	357.6
Total rainfall mm	86.2	68.0	84.0	410.4	69.4	117.4	835.4

Table 2. Characteristics of throughfall rainfall intensity, raindrop indices (*KE*, *M*, *MD*) of throughfall, and soil detachment rate in each observation period.

Period		I	II	III	IV	V	VI	Overall
Date in 2005		1 Jul – 7 Jul	8 Jul– 15 Jul	16 Jul– 26 Aug	27 Aug– 13 Sep	14 Sep– 3 Nov	4 Nov– 28 Nov	
I, rainfall intensity								
Total	mm	86.2	68.0	84.0	410.4	69.4	117.4	835.4
Max. (24-h)	mm h^{-1}	2.4	2.3	1.7	8.8	0.7	4.1	8.8
Max. (3-h)		7.4	7.4	4.3	16.8	3.1	8.9	16.8
Max. (1-h)		15.6	13.8	9.2	19.8	8.0	12.0	19.8
Max. (30-min)		29.6	19.6	14.8	25.6	14.4	14.0	29.6
Max. (10-min)		68.4	38.4	22.8	51.6	28.8	25.2	68.4
KE, kinetic energy								
Total	J m^{-2}	1415.1	1116.4	1379.0	6737.5	1139.3	1927.4	13714.8
Max. (24-h)	J m^{-2} h^{-1}	39.3	38.4	28.2	143.9	11.1	67.0	143.9
Max. (3-h)		121.5	121.5	70.0	275.8	51.4	146.7	275.8
Max. (1-h)		256.1	226.6	151.0	325.1	131.3	197.0	325.1
Max. (30-min)		485.9	321.8	243.0	420.3	236.4	229.8	485.9
Max. (10-min)		1122.9	630.4	374.3	847.1	472.8	413.7	1122.9
M, momentum								
Total	kg m s^{-1} m^{-2}	473.0	373.1	460.9	2251.9	380.8	644.2	4583.9
Max. (24-h)	kg m s^{-1} m^{-2} h^{-1}	13.1	12.8	9.4	48.1	3.7	22.4	48.1
Max. (3-h)		40.6	40.6	23.4	92.2	17.2	49.0	92.2
Max. (1-h)		85.6	75.7	50.5	108.6	43.9	65.8	108.6
Max. (30-min)		162.4	107.5	81.2	140.5	79.0	76.8	162.4
Max. (10-min)		375.3	210.7	125.1	283.1	158.0	138.3	375.3
MD, momentum multiplied by the drop diameter								
Total	kg m s^{-1} mm m^{-2}	2386.1	1615.3	1951.1	10502.0	1303.6	2807.6	20565.8
Max. (24-h)	kg m s^{-1} mm m^{-2} h^{-1}	63.1	58.1	41.7	247.1	14.2	102.0	247.1
Max. (3-h)		212.7	211.7	108.1	526.7	82.0	234.3	526.7
Max. (1-h)		635.4	448.6	263.9	654.5	243.3	334.7	654.5
Max. (30-min)		1246.0	683.0	455.7	977.0	470.1	432.0	1246.0
Max. (10-min)		3197.5	1508.4	765.4	2215.7	1037.3	871.9	3197.5
Detachment rate								
Mean	g m^{-2}	955.7	546.6	248.7	1034.1	107.1	322.3	3214.5
Standart deviation	g m^{-2}	712.3	375.7	163.6	682.1	77.7	237.8	1436.9

Table 3. Pearson's product-moment correlation coefficient and two-sided p-value between rainfall erosivity indices and soil splash detachment rates.

	I, KE, M		MD		EI_{30}	
	r	*p*	*r*	*p*	*r*	*p*
Total	0.632	0.178	0.674	0.142	0.688	0.131
Max. value						
24-h	0.676	0.140	0.692	0.128	—	—
3-h	0.764	0.077	0.783	0.066	—	—
1-h	0.954	0.003	0.995	0.000	—	—
30-min	0.948	0.004	0.924	0.008	—	—
10-min	0.897	0.015	0.888	0.018	—	—